

# Quantification of noise in the bi-functionality induced post-translational modification

Alok Kumar Maity,<sup>1</sup> Arnab Bandyopadhyay,<sup>2</sup> Sudip Chattopadhyay,<sup>3</sup> Jyotipratim Ray Chaudhuri,<sup>4</sup> Ralf Metzler,<sup>5,6</sup> Pinaki Chaudhuri,<sup>1</sup> and Suman K Banik<sup>2</sup>

<sup>1</sup>*Department of Chemistry, University of Calcutta, 92 A P C Road, Kolkata 700 009, India*

<sup>2</sup>*Department of Chemistry, Bose Institute, 93/1 A P C Road, Kolkata 700 009, India*

<sup>3</sup>*Department of Chemistry, Bengal Engineering and Science University, Shibpur, Howrah 711103, India*

<sup>4</sup>*Department of Physics, Katwa College, Katwa, Burdwan 713130, India*

<sup>5</sup>*Institute for Physics & Astronomy, University of Potsdam, D-14476 Potsdam-Golm, Germany*

<sup>6</sup>*Physics Department, Tampere University of Technology, FI-33101 Tampere, Finland*

(Dated: November 2, 2012)

We present a generic analytical scheme for the quantification of fluctuations due to bi-functionality induced signal transduction within the members of bacterial two-component system. The proposed model takes into account post-translational modifications in terms of elementary phosphotransfer kinetics. Sources of fluctuations due to autophosphorylation, kinase and phosphatase activity of the sensor kinase have been considered in the model via Langevin equations, which are then solved exactly within the framework of linear noise approximation. The resultant analytical expression of phosphorylated response regulators are then used to quantify the noise profile of biologically motivated single and branched pathways. Enhancement and reduction of noise in terms of extra phosphate outflux and influx, respectively, have been analyzed for the branched system.

PACS numbers: 87.18.Mp, 87.18.Tt, 87.18.Vf

## I. INTRODUCTION

The response of living systems in presence of an external stimulus is coordinated by highly specialized signal transduction machinery. In the bacterial kingdom this is achieved by the well characterized two-component system (TCS) minimally comprised of the membrane bound sensor kinase (SK) and the cytoplasmic response regulator (RR) [1–3]. The machinery of TCS is utilized by the bacteria to process the information of external signals in terms of phosphotransfer kinetics. When applied, an external stimulus causes phosphorylation at the histidine residue of SK which then gets transferred to the cognate (and/or non-cognate) RR at their aspartate domain. The phosphorylated RR then acts as a transcription factor for several downstream genes, as well as for the activation/repression of its own operon. It is now a well established fact that in addition to being a source (kinase), a SK can equally act as a sink (phosphatase) while interacting with a RR. Such bi-functional behavior of a SK towards RR can altogether build a robust motif in the bacterial signal transduction network [4–7].

Expression of proteins in individual cell is usually driven by the fluctuations present within the cellular environment as well as the fluctuations imposed by the external stimulus [8–14]. This often leads to variability in the expression level within the context of single cell [15–18]. When observed in the bulk such fluctuations gets averaged out over the cellular population. The prevalent fluctuations, whether external or internal, do not only effect the dynamics of gene expression it plays a major role in post-translational modification as well [19, 20]. In this connection it is also important to mention the role of cellular fluctuations in the different signal transduction motif that primarily uses phosphotransfer mecha-

nism. Using a push-pull amplifier loop mechanism theoretical study has been made to analyze the signal transduction within the photoreceptor of retina [21]. Theoretical model has been proposed to study the effect of reversibility in the phosphorylation-dephosphorylation cycle that can generate bistable behavior in the presence of noise and can propagate within the signaling cascade [22]. In the context of robustness in bacterial chemotaxis, reversibility on a signaling cascade has been shown to exert a stabilizing effect of adaptation through methylation [23]. Correlation between extrinsic and intrinsic noise that arises due to external signal and internal biochemical pathways, respectively, has been reported to enhance the robustness of zero-order ultrasensitivity [24].

Post-translational modification in terms of phosphate transfer is important to generate the pool of phosphorylated RR that act as a transcription factor for several downstream genes. Bi-functionality on the other hand plays a crucial role to maintain this pool as the information flows through the phosphotransfer motif. Thus bi-functionality and post-translational modification works hand in hand to maintain the optimal pool of phosphorylated RR. Since this composite functional behavior take place in a noisy cellular environment it is worthwhile to investigate the role of cellular noise on the bi-functionality controlled post-translational modification of the components of the well composed signal transduction machinery. The specific question we aim to address here is how the cellular fluctuations affect this functional motif or in a noisy environment whether individual cell can maintain bi-functionality while generating optimal level of noise? To address this questions we develop in the present communication a generic mathematical model to study the role of molecular noise on the post-translational modification of system components and on

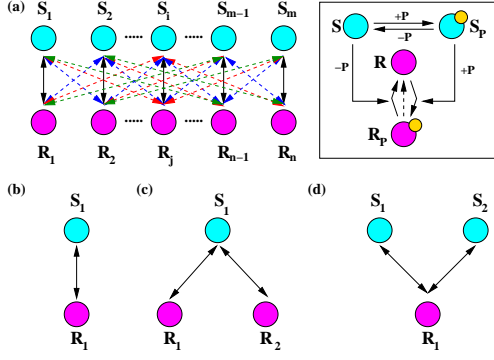


FIG. 1. (color online) The wiring diagrams for the proposed post-translational interactions between SK and RR. The cyan and magenta blob stands for the SK and RR, respectively. (a) The generalized  $m:n$  system with cognate (solid black arrow) and non-cognate (dashed colored arrow) kinase and phosphatase interactions. (b), (c) and (d) are wiring diagram for 1:1, 1:2 and 2:1 interactions, respectively. The boxed wiring diagram depicts the phosphate addition (+P) and removal (-P) kinetics between a pair of cognate and/or non-cognate SK and RR that ultimately results into phosphorylated RR (magenta blob with a yellow blob on top). The dotted arrowhead is for auto-dephosphorylation of RR. For simplicity we do not show the yellow blob in (a)-(d).

the bi-functionality of the signal transduction machinery of bacterial TCS.

## II. THE MODEL

We start by considering a simple system describing post-translational modification due to phosphotransfer mechanism of a typical TCS, where  $m$  numbers of SK interacts with  $n$  numbers of RR, the ultimate product of which is  $R_p$ , the phosphorylated RR. We call the proposed model as the  $m:n$  system (Fig. 1a) where each of the SK, RR and their phosphorylated forms are designated as  $S$ ,  $R$ ,  $S_p$  and  $R_p$ , respectively. The generic model we consider here involves single pair interaction (Fig. 1b). In addition it takes care of *branched pathways* [3]; for example the 1:2 system (Fig. 1c) mimics the *one to many* pathway as observed in chemotaxis system in *E. coli*, where the SK CheA phosphorylates two RR, CheY and CheB [25]. Similarly the 2:1 system (Fig. 1d) follows the kinetics of *many to one* pathway as observed in *V. cholerae* where the SK LuxS and CqsS phosphorylate the RR LuxO [26], respectively.

As mentioned earlier, in typical bacterial TCS the key steps of phosphotransfer mechanism involve autophosphorylation at SK, transfer of phosphate group from SK to RR, and SK mediated removal of phosphate group from RR (see boxed diagram in Fig. 1). To keep the model simple we do not consider the synthesis (birth) or degradation (death) of any system component. The interaction we consider here may be of cognate and/or

non-cognate type. Out of the  $m:n$  pair one can consider the specific interaction between  $i$ -th SK and  $j$ -th RR, where  $1 \leq i \leq m$  and  $1 \leq j \leq n$ , to write down the elementary kinetic steps considering the minimal interaction between a specific pair

$$S_i \xrightleftharpoons[k_{-i}]{k_i} S_{pi}, \quad (1a)$$

$$S_{pi} + R_j \xrightarrow{k_{kij}} S_i + R_{pj}, \quad (1b)$$

$$S_i + R_{pj} \xrightarrow{k_{pij}} S_i + R_j. \quad (1c)$$

$$R_{pj} \xrightarrow{k_{apj}} R_j. \quad (1d)$$

In the above kinetic steps, Eq. (1a) considers autophosphorylation at the histidine residue of the SK. Generally, autophosphorylation takes place under the influence of an external signal [1–3] which we consider to be of constant type and have been absorbed in the rate constant  $k_i$ . Eqs. (1b-1c) takes into account the kinase and phosphatase activity of the SK, respectively, thus considering the bi-functional behavior of the SK. Eq. (1d) denotes the auto-dephosphorylation of the RR independent of the phosphatase effect of SK on RR [6].

Due to the inherent noisy nature of the cellular environment each of the four reactions mentioned above are influenced by fluctuations and in turn affect the copy numbers of each system component. To take this into account we introduce Langevin noise terms that can influence each of the reactions independently given by Eqs. (1a-1d). The interaction of a single SK with multiple RR or *vice versa* in presence of fluctuations we consider here can be compared with stochastic system-reservoir formalism where a single system interacts with multiple reservoir or *vice versa* [27]. In terms of phosphate transfer, SK pumps in energy to RR when act as kinase, whereas the same withdraws energy from RR while acting as phosphatase. The stochastic differential equations describing the phosphorylated SK and RR in presence of fluctuations can be written as

$$\begin{aligned} \frac{dS_{pi}}{dt} = & k_i(S_{Ti} - S_{pi}) - k_{-i}S_{pi} - \sum_{j=1}^n k_{kij}S_{pi} \\ & \times (R_{Tj} - R_{pj}) + \xi_i(t) \end{aligned} \quad (2a)$$

$$\begin{aligned} \frac{dR_{pj}}{dt} = & \sum_{i=1}^m k_{kij}S_{pi}(R_{Tj} - R_{pj}) - \sum_{i=1}^m [k_{pij} \\ & \times (S_{Ti} - S_{pi}) + k_{apj}]R_{pj} + \psi_j(t). \end{aligned} \quad (2b)$$

Here  $S_{Ti} = S_i + S_{pi}$  and  $R_{Tj} = R_j + R_{pj}$  stand for the total amount of  $i$ -th SK and  $j$ -th RR, respectively. The noise terms  $\xi_i$  and  $\psi_j$  take care of the fluctuations in the copy number of  $S_{pi}$  and  $R_{pj}$ , respectively. Within the framework of linear noise approximation we define the statistical properties of the Langevin terms obeying the fluctuation-dissipation relation [20, 28–30] with zero

mean,  $\langle \xi_i(t) \rangle = \langle \psi_j(t) \rangle = 0$  and

$$\begin{aligned}\langle \xi_i(t) \xi_i(t + \tau) \rangle &= 2k_i(S_{Ti} - S_{Pi})\delta(\tau), \\ \langle \psi_j(t) \psi_j(t + \tau) \rangle &= 2 \sum_{i=1}^m k_{kij} S_{pi} (R_{Tj} - R_{pj}) \delta(\tau),\end{aligned}$$

with  $\langle S_{pi} \rangle$  and  $\langle R_{pj} \rangle$  being the mean values at the steady state. In addition, we consider both the noise terms are correlated [24, 31]

$$\langle \xi_i(t) \psi_j(t + \tau) \rangle = -k_{kij} S_{pi} (R_{Tj} - R_{pj}) \delta(\tau).$$

Linearizing Eqs. (2a-2b) around the steady state, i.e.,  $S_{pi} = \langle S_{pi} \rangle + \delta S_{pi}$  and  $R_{pj} = \langle R_{pj} \rangle + \delta R_{pj}$ , we have

$$\begin{aligned}\frac{d}{dt} \begin{pmatrix} \delta S_{pi} \\ \delta R_{pj} \end{pmatrix} &= \begin{pmatrix} -a_i & \sum_{j=1}^n k_{kij} \langle S_{pi} \rangle \\ \sum_{i=1}^m b_{ij} & -c_j \end{pmatrix} \\ &\times \begin{pmatrix} \delta S_{pi} \\ \delta R_{pj} \end{pmatrix} + \begin{pmatrix} \xi_i \\ \psi_j \end{pmatrix},\end{aligned}\quad (3)$$

where

$$\begin{aligned}a_i &= \frac{k_i S_{Ti}}{\langle S_{pi} \rangle}, b_{ij} = (k_{pij} S_{Ti} + k_{apj}) \frac{\langle R_{pj} \rangle}{\langle S_{pi} \rangle}, \\ c_j &= \sum_{i=1}^m \frac{[k_{pij} (S_{Ti} - \langle S_{pi} \rangle) + k_{apj}] R_{Tj}}{R_{Tj} - \langle R_{pj} \rangle}.\end{aligned}$$

Solving Eq. (3) and performing Fourier transformation  $\delta \tilde{X}(\omega) = \int_{-\infty}^{\infty} \delta X(t) e^{-i\omega t} dt$  on the resultant solution we have in matrix notation the generalized solution for both  $\delta \tilde{S}_p(\omega)$  and  $\delta \tilde{R}_p(\omega)$ ,

$$\delta \tilde{\mathbf{S}}_p(\omega) = \mathbf{A}^{-1} (\langle \mathbf{S}_{pK} \rangle \delta \tilde{\mathbf{R}}_p(\omega) + \tilde{\boldsymbol{\xi}}(\omega)), \quad (4a)$$

$$\delta \tilde{\mathbf{R}}_p(\omega) = \mathbf{P}^{-1} (\mathbf{B}^T \mathbf{A}^{-1} \tilde{\boldsymbol{\xi}}(\omega) + \tilde{\boldsymbol{\psi}}(\omega)), \quad (4b)$$

where  $\mathbf{P} = \mathbf{C} - \mathbf{B}^T \mathbf{A}^{-1} \langle \mathbf{S}_{pK} \rangle$ . In the above expressions (4a-4b),  $\delta \tilde{\mathbf{S}}_p$  and  $\delta \tilde{\mathbf{R}}_p$  are  $m \times 1$  and  $n \times 1$  dimensional column vectors with elements  $\delta \tilde{S}_{pi}$  and  $\delta \tilde{R}_{pj}$ , respectively. Likewise,  $\tilde{\boldsymbol{\xi}}$  and  $\tilde{\boldsymbol{\psi}}$  are  $m \times 1$  and  $n \times 1$  column vectors with elements  $\tilde{\xi}_i$  and  $\tilde{\psi}_j$ , respectively.  $\mathbf{A}$  and  $\mathbf{C}$  are diagonal matrix of order  $m \times m$  and  $n \times n$  with elements  $(i\omega + a_i)$  and  $(i\omega + c_j)$ , respectively. Additionally,  $\langle \mathbf{S}_{pK} \rangle$  and  $\mathbf{B}$  are matrix of order  $m \times n$  with elements  $\langle S_{pi} \rangle k_{kij}$  and  $b_{ij}$ , respectively.

Since we are interested in the effect of noise on phosphorylated RR,  $R_p$ , which acts as transcription factor for one or more genes including the gene that encodes SK and RR we now focus on the solution of Eq. (4b) only. From the structure of Eq. (4b) it is clear that dynamics of  $R_p$  is now decoupled from  $S_p$ . To understand the role of fluctuations in phosphotransfer processes, we define the quantity noise at steady state,  $\eta_{R_p} = \sigma_{R_p} / \langle R_p \rangle$ . While calculating the noise for the three different systems (1:1, 1:2 and 2:1) mentioned in Fig. (1) we only focus on the noise level of  $R_{p1}$ , the phosphorylated form of  $R_1$ . Noise generated due to other interactions ( $S_1$  and  $R_2$ , and  $S_2$  and  $R_1$ ) are considered to add extra layers of information

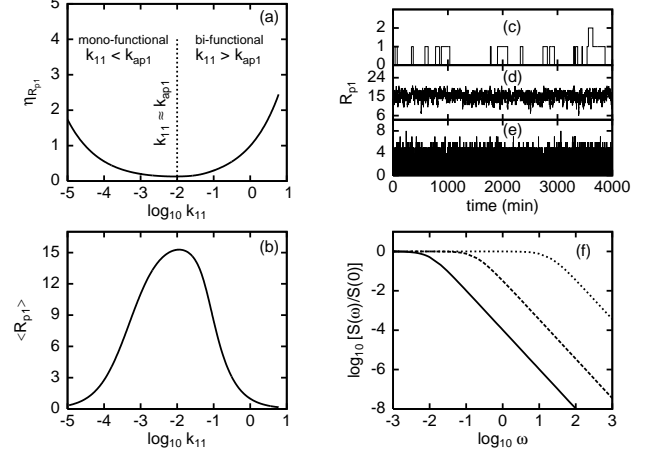


FIG. 2. Plot of noise, steady state protein level, time series and power spectra for 1:1 system. (a) Noise  $\eta_{R_{p1}}$  as a function of  $\log_{10} k_{11}$ . The noise profile has been shown to contain three different regions, viz mono-functional region ( $k_{11} < k_{ap1}$ ), crossover region ( $k_{11} \approx k_{ap1}$ ) and bi-functional region ( $k_{11} > k_{ap1}$ ). In the absence of auto-dephosphorylation kinetics (Eq. (1d)) only the bi-functional domain exists, whereas in the absence of phosphatase kinetics (Eq. (1c)) only the mono-functional domain becomes prevalent. (b) Steady state  $R_{p1}$  as a function of  $\log_{10} k_{11}$ . (c)-(e) Time series of  $R_{p1}$  for low ( $k_{11} = 10^{-5}$ ), intermediate ( $k_{11} = 10^{-2}$ ) and high ( $k_{11} = 1$ ) values of  $k_{11}$ , respectively, generated using Gillespie algorithm [32, 33] (f) Normalized power spectra for low (solid line), intermediate (dashed line) and high (dotted line) values of  $k_{11}$ . In all the cases  $k_1/k_{-1} = 5$ ,  $k_{ap1} = 0.01$  and  $S_{T1} = R_{T1} = 20$ .

on the noise profile of  $R_{p1}$ . During the calculation of noise and power spectra we have considered  $k_{kij} = k_{pij} = k_{ij}$  ( $i, j = 1, 2$ ), as kinase and phosphatase activity between SK and RR takes place via protein-protein interaction. It is important to note that while interacting with its partner a SK shows both mono-functional and bi-functional behavior for  $k_{apj} > k_{ij}$  and  $k_{apj} < k_{ij}$ , respectively [6]. At  $k_{apj} \approx k_{ij}$  (cross over regime) system makes transition from mono- to bi-functional domain.

### III. RESULTS AND DISCUSSION

In Fig. (2a) noise profile of  $R_{p1}$  has been shown in a semilog plot. For 1:1 system at a low value of  $k_{11}$  noise has a nonzero value which goes down as  $k_{11}$  value increases. As  $k_{11}$  value increases further noise increases and reaches a higher value. As evident from the definition, noise is inversely proportional to the population of steady state  $R_{p1}$ . To check the role of  $\langle R_{p1} \rangle$  on steady state noise we have calculated  $\langle R_{p1} \rangle$  as a function of  $\log_{10} k_{11}$  (Fig. 2b) from which it is clear that the protein profile develops exactly in the opposite way of the noise profile and imparts an inverse effect on the noise development.

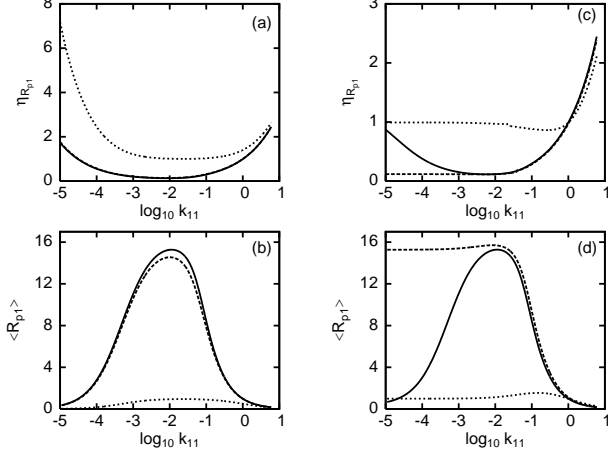


FIG. 3. Plot of noise and steady state protein level for branched (1:2 and 2:1) pathways. (a,c) Noise profile for 1:2 and 2:1 system, respectively, as a function of  $\log_{10} k_{11}$ . The solid, dashed and dotted lines are for low ( $10^{-5}$ ), intermediate ( $10^{-2}$ ) and high (1) values of  $k_{12}$  (for 1:2) and  $k_{21}$  (for 2:1). (b,d) Steady state level of  $R_{p1}$  for the same values of  $k_{12}$  and  $k_{21}$  as in (a,c). For all the cases  $k_i/k_{-i} = 5$ ,  $k_{apj} = 0.01$  and  $ST_i = R_{Tj} = 20$ .

For the low value of  $k_{11}$  the auto-dephosphorylation  $k_{ap1}$  dominates over the phosphatase activity of SK on RR ( $k_{11} < k_{ap1}$ ). In this regime the sensor shows mono-functional activity by acting as a kinase only, which is still lower than  $k_{ap1}$ . This effectively reduces the  $R_{p1}$  level (Fig. 2c) and increases the noise of the system. In the limit  $k_{11} \approx k_{ap1}$  (vertical dotted line in Fig. 2a)  $R_{p1}$  level reaches at its maximum (Fig. 2b and Fig. 2d) while reducing the noise. When  $k_{11}$  exceeds  $k_{ap1}$  ( $k_{11} > k_{ap1}$ ), the phosphatase activity of SK starts to show up in addition to its kinase activity. In this regime bi-functional property of SK comes into play reducing the copy of  $R_{p1}$  (Fig. 2e) henceforth increasing the noise of the system. To understand how the system relaxes under the influence of the protein protein interaction, we calculate the power spectra  $S(\omega) = \langle \delta \tilde{R}_{p1}(\omega) \delta \tilde{R}_{p1}(\omega') \rangle$  (Fig. 2f). The resultant spectral lines are plotted for low, intermediate and high  $k_{11}$  ( $= k_{k11} = k_{p11}$ ) values. As expected the power spectra relaxes faster for low  $k_{11}$  value compared to intermediate  $k_{11}$  value which again relaxes faster compared to higher  $k_{11}$  value. For a low value of  $k_{11}$  the conversion of  $R$  into  $R_p$  is a slow process and hence fast fluctuations in the copy number have minimal effect on the power spectrum. As  $k_{11}$  value increases the conversion rate increases and thus gets affected by the noise in the copy number which results into slower relaxation.

In Figs. (3a-3c) in a semilog plot we show the noise,  $\eta_{R_{p1}}$  for 1:2 and 2:1 system as a function of  $k_{11}$ . For comparison we refer to noise profile of 1:1 system shown in Fig. (2a). In 1:2 system a single SK,  $S_1$  interacts

with two RR,  $R_1$  and  $R_2$ , with its bifunctional properties acting on both the RRs. In Fig. (3a) we show the noise generated for  $R_{p1}$  while taking into account the kinase and phosphatase rates ( $k_{k12} = k_{p12} = k_{12}$ ) between  $S_1$  and  $R_2$  to be low ( $k_{12} = 10^{-5}$ ), intermediate ( $k_{12} = 10^{-2}$ ) and high ( $k_{12} = 1$ ). For low and intermediate  $k_{12}$  value the noise profile looks almost like 1:1 system as  $k_{11}$  is varied. This happens as interaction between  $S_1$  and  $R_2$  adds a weak layer of information on  $R_1$  due to mono-functional property of  $S_1$  on  $R_2$  ( $k_{ap2} \geq k_{12}$ ). Whereas for high  $k_{12}$  value a huge amplification of noise occurs (the dotted line in Fig. (3a)). In this domain as  $k_{ap2} < k_{12}$ , SK starts to show its bi-functional property and is more active in its interaction with  $R_2$ , rather than with  $R_1$ . Such active interaction between  $S_1$  and  $R_2$  adds an extra layer of outflux of phosphate group from  $R_1$  (the dotted line in Fig. 3b) thus leading to low level of  $\langle R_{p1} \rangle$  and enhancement of noise.

In 2:1 system a single RR,  $R_1$  interacts with two SK,  $S_1$  and  $S_2$ . In Fig. (3c) we show the noise generated for  $R_{p1}$  while taking into account the kinase and phosphatase rates ( $k_{k21} = k_{p21} = k_{21}$ ) between  $S_2$  and  $R_1$  to be low ( $k_{21} = 10^{-5}$ ), intermediate ( $k_{21} = 10^{-2}$ ) and high ( $k_{21} = 1$ ). For low value of  $k_{21}$  the noise profile is similar to that one for 1:1 system as  $k_{11}$  is increased. Although in this domain  $S_2$  acts as kinase only, it provides a low level of input on  $R_1$  as  $k_{ap1} > k_{21}$ . Interesting behavior emerges as  $k_{21}$  takes intermediate and high value. In the intermediate domain maximal level of  $\langle R_{p1} \rangle$  is produced due to extra influx of phosphate group. This large influx due to  $k_{21}$  can overpower the low kinase effect of  $k_{11}$ , henceforth increases the steady state level of  $R_{p1}$  as a effect of which the noise level attains a minimum value. For high  $k_{21}$ ,  $k_{ap1} < k_{21}$  where  $S_2$  starts to show its bi-functional property via phosphate input and removal. This helps the composite system to maintain a high value of noise for a wide range. Note that, compared to the low and intermediate domain the protein level in this region goes down drastically due to strong phosphatase activity of  $S_2$  on  $R_1$ . It is interesting to note that for intermediate and high  $k_{21}$  value the composite system loses its mono-functional behavior almost completely (Fig. 3d).

#### IV. CONCLUSION

To conclude, we have provided a generic description for the calculation of noise due to post-translational modification in bacterial TCS. From exact analytical calculation within the purview of linear noise approximation it is possible to quantify the steady state noise for a single pair and branched pathways. For single pair system our analysis shows the effect of bi-functionality of SK on noise generation and could differentiate the mono- and bi-functional domain in the noise profile. Calculation for branched pathways shows enhancement and reduction of noise for the composite system in terms of extra phosphate outflux and influx, respectively. Our analysis sug-

gests that in *one to many* system as in the chemotaxis pathway of *E. coli* enhancement of fluctuations happens due to extra outflux of phosphate group within the members of TCS. On the other case, for *many to one* system mimicking the quorum sensing network of *V. cholerae* an optimal level of noise can be maintained via extra influx of phosphate group. To maintain such low noise activity SK of *V. cholerae* phosphotransfer circuit might prefer to operate in the cross over domain.

## ACKNOWLEDGMENTS

AKM and AB are thankful to UGC (UGC/776/JRF(Sc)) and CSIR (09/015(0375)/2009-

EMR-I), respectively, for research fellowship. RM acknowledges funding through the Academy of Finland's FiDiPro scheme. PC wishes to thank The Centre for Research on Nano Science and Nano Technology, University of Calcutta for a research grant [Conv/002/Nano RAC (2008)]. SKB acknowledges support from Bose Institute through Institutional Programme VI - Development of Systems Biology.

- 
- [1] J. L. Appleby, J. S. Parkinson, and R. B. Bourret, *Cell* **86**, 845 (1996).
  - [2] J. A. Hoch, *Curr Opin Microbiol* **3**, 165 (2000).
  - [3] M. T. Laub and M. Goulian, *Annu Rev Genet* **41**, 121 (2007).
  - [4] E. Batchelor and M. Goulian, *Proc Natl Acad Sci U S A* **100**, 691 (2003).
  - [5] G. Shinar, R. Milo, M. R. Martínez, and U. Alon, *Proc Natl Acad Sci U S A* **104**, 19931 (2007).
  - [6] A. Siryaporn, B. S. Perchuk, M. T. Laub, and M. Goulian, *Mol Syst Biol* **6**, 452 (2010).
  - [7] A. H. West and A. M. Stock, *Trends Biochem Sci* **26**, 369 (2001).
  - [8] A. Eldar and M. B. Elowitz, *Nature* **467**, 167 (2010).
  - [9] M. B. Elowitz, A. J. Levine, E. D. Siggia, and P. S. Swain, *Science* **297**, 1183 (2002).
  - [10] B. Munsky, G. Neuert, and A. van Oudenaarden, *Science* **336**, 183 (2012).
  - [11] J. Paulsson, *Nature* **427**, 415 (2004).
  - [12] N. Rosenfeld, J. W. Young, U. Alon, P. S. Swain, and M. B. Elowitz, *Science* **307**, 1962 (2005).
  - [13] R. Silva-Rocha and V. de Lorenzo, *Annu Rev Microbiol* **64**, 257 (2010).
  - [14] M. Thattai and A. van Oudenaarden, *Proc Natl Acad Sci U S A* **98**, 8614 (2001).
  - [15] C. J. Davidson and M. G. Surette, *Annu Rev Genet* **42**, 253 (2008).
  - [16] R. Losick and C. Desplan, *Science* **320**, 65 (2008).
  - [17] E. Rotem, A. Loinger, I. Ronin, I. Levin-Reisman, C. Gabay, N. Shores, O. Biham, and N. Q. Balaban, *Proc Natl Acad Sci U S A* **107**, 12541 (2010).
  - [18] K. Sureka, B. Ghosh, A. Dasgupta, J. Basu, M. Kundu, and I. Bose, *PLoS One* **3**, e1771 (2008).
  - [19] T. Jia and R. V. Kulkarni, *Phys Rev Lett* **105**, 018101 (2010).
  - [20] P. Mehta, S. Goyal, and N. S. Wingreen, *Mol Syst Biol* **4**, 221 (2008).
  - [21] P. B. Detwiler, S. Ramanathan, A. Sengupta, and B. I. Shraiman, *Biophys J* **79**, 2801 (2000).
  - [22] C. A. Miller and D. A. Beard, *Biophys J* **95**, 2183 (2008).
  - [23] U. Alon, M. G. Surette, N. Barkai, and S. Leibler, *Nature* **397**, 168 (1999).
  - [24] S. Tănase-Nicola, P. B. Warren, and P. R. ten Wolde, *Phys Rev Lett* **97**, 068102 (2006).
  - [25] J. P. Armitage, *Adv Microb Physiol* **41**, 229 (1999).
  - [26] C. M. Waters and B. L. Bassler, *Annu Rev Cell Dev Biol* **21**, 319 (2005).
  - [27] A. V. Popov and R. Hernandez, *J Chem Phys* **126**, 244506 (2007).
  - [28] W. Bialek and S. Setayeshgar, *Proc Natl Acad Sci U S A* **102**, 10040 (2005).
  - [29] J. Elf and M. Ehrenberg, *Genome Res* **13**, 2475 (2003).
  - [30] N. G. van Kampen, *Stochastic Processes in Physics and Chemistry* (North-Holland, Amsterdam, 2005).
  - [31] P. S. Swain, *J Mol Biol* **344**, 965 (2004).
  - [32] D. T. Gillespie, *J Comp Phys* **22**, 403 (1976).
  - [33] D. T. Gillespie, *J Phys Chem* **81**, 2340 (1977).